Fungal Genetics and Biology 46 (2009) 956–963

Contents lists available at ScienceDirect

Fungal Genetics and Biology

journal homepage: www.elsevier.com/locate/yfgbi

Cryptococcus neoformans cryoultramicrotomy and vesicle fractionation reveals an intimate association between membrane lipids and glucuronoxylomannan

Débora L. Oliveira [a], Leonardo Nimrichter [a], Kildare Miranda [b], Susana Frases [c,d,1], Kym F. Faull [e], Arturo Casadevall [c,d,2], Marcio L. Rodrigues [a,*,2]

[a] *Laboratorio de Estudos Integrados em Bioquimica Microbiana, Instituto de Microbiologia Professor Paulo de Goes, Universidade Federal do Rio de Janeiro, Rio de Janeiro 21941590, Brazil*
[b] *Laboratorio de Ultraestrutura Celular Hertha Meyer, Instituto de Biofisica Carlos Chagas Filho, Universidade Federal do Rio de Janeiro, Rio de Janeiro 21941590, Brazil*
[c] *Department of Medicine, Albert Einstein College of Medicine, 1300 Morris Park Ave., Bronx, NY 10461, USA*
[d] *Departments of Microbiology and Immunology, Albert Einstein College of Medicine, 1300 Morris Park Ave., Bronx, NY 10461, USA*
[e] *Pasarow Mass Spectrometry Laboratory, Semel Institute for Neuroscience and Human Behavior and the Department of Psychiatry and Biobehavioral Sciences, David Geffen School of Medicine, University of California, Los Angeles, CA 90095, USA*

ARTICLE INFO

Article history:
Received 3 August 2009
Accepted 2 September 2009
Available online 10 September 2009

Keywords:
Cryptococcus neoformans
GXM transport
Secretory vesicles
Cryoimmunoelectronmicroscopy

ABSTRACT

Cryptococcus neoformans is an encapsulated pathogenic fungus. The cryptococcal capsule is composed of polysaccharides and is necessary for virulence. It has been previously reported that glucuronoxylomannan (GXM), the major capsular component, is synthesized in cytoplasmic compartments and transported to the extracellular space in vesicles, but knowledge on the organelles involved in polysaccharide synthesis and traffic is extremely limited. In this paper we report the GXM distribution in *C. neoformans* cells sectioned by cryoultramicrotomy and visualized by transmission electron microscopy (TEM) and polysaccharide immunogold staining. Cryosections of fungal cells showed high preservation of intracellular organelles and cell wall structure. Incubation of cryosections with an antibody to GXM revealed that cytoplasmic structures associated to vesicular compartments and reticular membranes are in close proximity to the polysaccharide. GXM was generally found in association with the membrane of intracellular compartments and within different layers of the cell wall. Analysis of extracellular fractions from cryptococcal supernatants by transmission electron microscopy in combination with serologic, chromatographic and spectroscopic methods revealed fractions containing GXM and lipids. These results indicate an intimate association of GXM and lipids in both intracellular and extracellular spaces consistent with polysaccharide synthesis and transport in membrane-associated structures.

1. Introduction

The most prominent feature of the fungal pathogen *Cryptococcus neoformans* is the presence of a capsule surrounding the yeast cell body. This structure is composed mainly of polysaccharides, including glucuronoxylomannan (GXM) and galactoxylomannan (GalXM) (Zaragoza et al., 2009). The cryptococcal capsule is crucial for fungal cell survival in different situations, including environmental interactions with predators (Steenbergen et al., 2001) or evasion of the immune system during human and animal infections (Monari et al., 2008; Vecchiarelli, 2007). GXM is considered the most important virulence factor of *C. neoformans* (McClelland et al., 2005) and, for this reason, it is also the most well studied structural component.

GXM biosynthesis involves several enzymatic steps, starting with sugar polymerization using nucleotide-activated sugar monomers as precursors (Wills et al., 2001; Zaragoza et al., 2009). In contrast to cell wall polysaccharides like chitin and glucans, which are most probably synthesized at plasma membrane level, GXM epitopes are found at intracellular sites (Feldmesser et al., 2001; Garcia-Rivera et al., 2004; Yoneda and Doering, 2006), that presumably reflect the sites of initial assembly. Mutation in the gene coding for a Rab/GTPase ortologue of the *Saccharomyces cerevisiae* Sec4p caused accumulation of cytoplasmic GXM-containing vesicles (Yoneda and Doering, 2006), raising the possibility that newly synthesized polysaccharides might be exported to the cell surface by vesicular traffic. Since Sec4p is involved in post-Golgi secretion

* Corresponding author.
E-mail addresses: marcio@micro.ufrj.br, marciolrodrig@gmail.com (M.L. Rodrigues).
[1] Present address: Instituto Nacional de Metrologia, Normalizacao e Qualidade Industrial, 50 Ave. NS das Gracas, Xerem 25259-020 Duque de Caxias, RJ, Brazil.
[2] These authors share senior authorship.

1087-1845/$ - see front matter © 2009 Elsevier Inc. All rights reserved.
doi:10.1016/j.fgb.2009.09.001

events, it was deduced that GXM was at least partially synthesized at the Golgi apparatus (Yoneda and Doering, 2006). GXM-containing vesicles are released to the extracellular milieu (Rodrigues et al., 2008, 2007) in a process that apparently involves the *SEC6* gene (Panepinto et al., 2009). Little is known about the biogenesis of extracellular GXM-containing vesicles. Although different studies suggest a role of genes related to conventional post-Golgi secretion in vesicle release (Panepinto et al., 2009; Yoneda and Doering, 2006), proteomic analysis of isolated *C. neoformans* vesicles reveled similarities with mammalian exosomes (Rodrigues et al., 2008).

Our knowledge on the steps of GXM biosynthesis and cellular traffic is limited by the paucity of information on its intracellular distribution. Previous ultrastructural analysis of *C. neoformans* cells by immunoelectron microscopy (IEM) revealed that antibodies raised against GXM recognize intracellular sites (Feldmesser et al., 2001; Garcia-Rivera et al., 2004; Yoneda and Doering, 2006, 2009). Conventional IEM procedures, however, include several steps of dehydration and embedding with different resins, which markedly affects preservation of the cell envelope and intracellular structures and organelles, and generates structural artifacts. Such subcellular modifications usually include loss of cytoplasmic content, poor preservation of membranous structures and cell wall shrinkage (Yamaguchi et al., 2005).

Cryoimmunogold labeling has been successfully used in different studies of the *C. neoformans* biology (Rodrigues et al., 2008, 2007, 2000). Using this technique, in which cells are promptly fixed, frozen and sectionated, the artifacts that can plague conventional IEM are reduced or avoided, and the result is superior preservation of subcellular structures, such as the nucleus, vacuoles and mitochondria. In addition, cryosectioning has been suggested to be the electron microscopy technique that is best suited for preserving cellular epitopes (Slot and Geuze, 2007).

In a previous study by our group, we used a cryoultramicrotomy protocol to study the cellular distribution of a glycolipid antigen in *C. neoformans* (Rodrigues et al., 2000). Well preserved cells were obtained, which allowed us to examine in detail different cellular structures, including the cell wall and membranous structures. In the present work, that method was used in association with vesicle isolation and lipid analysis for the study of the distribution of GXM in *C. neoformans*. Our data revealed that the polysaccharide is associated with lipid matrices and previously unknown subcellular and extracellular structures, indicating that GXM traffic in *C. neoformans* involves still unclear cellular events that may include unconventional steps of secretion.

2. Material and methods

2.1. Fungal cells

C. neoformans strain H99 was grown in minimal medium composed of dextrose (15 mM), $MgSO_4$ (10 mM), KH_2PO_4 (29.4 mM), glycine (13 mM), and thiamine-HCl (3 μM). Fungal cells were cultivated with shaking in Erlenmeyer flasks at 30 °C for 72 h. Cells were collected by centrifugation and then processed for IEM.

2.2. Electron microscopy

Electron microscopy procedures were based on the studies by Tokuyasu (1973) and Rodrigues and colleagues (2000)). The cells were fixed in 0.1 M sodium cacodylate buffer (pH 7.2) containing 4% paraformaldehyde, 0.2% glutaraldehyde, and 1% picric acid for 60 min at room temperature. The cells were then washed three times in PBS, infiltrated in gelatin, cut into cubes of 1 mm and infiltrated in 25% polyvinylpyrrolidone (PVP) and 2.3 M sucrose overnight in a cold room. The polyvinylpyrrolidone embedded blocks were then mounted on cryoultramicrotome stubs and flash frozen by immersion in liquid nitrogen. After trimming, ultrathin cryosections were obtained at a temperature of −130 °C using an Ultracut UCT cryoultramicrotome (Reichert). Flat ribbons of sections were shifted from the knife edge with an eyelash and picked up in a wire loop filled with a drop of 1% (w/v) methyl cellulose, 2.3 M sucrose in PBS buffer. Sections were thawed on the pickup droplet and transferred, sections downwards, to Formvar carbon-coated nickel grids.

For immunolabelling, grids were passed over a series of droplets of washing and were blocked in PBS-bovine serum albumin 1%. After blocking the cryosections were incubated overnight in the presence of 1 μg/ml of the murine monoclonal antibody (mAb) to GXM 18B7, washed again and incubated for 1 h with 15 nm (particle size) gold-labeled anti-mouse IgG. In control systems, the cryosections were incubated with PBS instead of the mAb 18B7, followed by the gold-labeled anti-mouse IgG. After a final washing series in PBS and distilled water, the sections were left for 15 min on 2% uranyl acetate (aqueous) and transferred to 0.75% methyl cellulose droplets. After 30 s, the grids were looped out, the excess viscous solution was drained away and the sections were allowed to dry. After drying, specimens were observed in a JEOL 1200EX transmission electron microscope operating at 80 kV.

Transmission electron microscopy was used to analyze the morphology and the integrity of extracellular vesicles isolated from culture supernatants. Pellets obtained after centrifugation of cell-free supernatants at 100,000*g* (see vesicle isolation and fractionation below) were fixed with 2% glutaraldehyde in 0.1 M cacodylate at room temperature for 2 h, and then incubated overnight in 4% formaldehyde, 1% glutaraldehyde, and 0.01 M PBS. The samples were incubated for 90 min in 2% osmium, serially dehydrated in ethanol, and embedded in Spurrs epoxy resin. Thin sections were obtained on a Reichart Ultracut UCT and stained with 0.5% uranyl acetate and 0.5% lead citrate. Samples were observed in a JEOL 1200EX transmission electron microscope operating at 80 kV.

2.3. Vesicle isolation and fractionation

Isolation of extracellular vesicles was based on a protocol described by Rodrigues et al. (2007). Cell-free culture supernatants were obtained by sequential centrifugation at 5000 and 15,000*g* (15 min, 4 °C) for removal of cells and debris. These supernatants were concentrated approximately 20-fold using an Amicon ultrafiltration system (cutoff 100 kDa). The concentrate was again sequentially centrifuged at 4000 and 15,000*g* (15 min, 4 °C) and the remaining supernatant was then ultracentrifuged at 100,000*g* for 1 h at 4 °C. The supernatant was discarded, and the pellet was washed by five sequential suspension and centrifugation steps, each consisting of 100,000*g* for 1 h at 4 °C with 0.1 M Tris-buffered saline. To remove extravesicular GXM contamination, vesicles were subjected to passage through a column packed with cyanogen bromide-activated Sepharose coupled to a monoclonal antibody to GXM, as described previously (Rodrigues et al., 2007). Ultracentrifugation pellets were finally fractionated in Optiprep gradients, as previously described for the analysis of virions and mammalian exosomes (Cantin et al., 2008). Optiprep gradients were prepared in PBS as 11 steps of 300 μl in 1.2% increments ranging from 6% to 18%. Vesicles were layered onto the top of the gradient and ultracentrifuged at 250,000*g* for 75 min. Eleven fractions of the gradient were collected from top to bottom. Each fraction was then analyzed for the presence of sterols and GXM.

2.4. Lipid analysis

The pellets obtained from centrifugation of cell supernatants at 100,000*g* were first suspended in methanol, and then two volumes

of chloroform were added. The mixture was vigorously vortexed and centrifuged to separate immediately formed polysaccharide-containing precipitates. The supernatant was removed, dried with a nitrogen stream, and partitioned according to Folch et al. (1957). The lower phase, containing neutral lipids, was recovered and dried by vacuum centrifugation. The dry residue was then prepared for phospholipid analysis by combined liquid chromatography–tandem mass spectrometry (LC/MS/MS) or sterol analysis by thin-layer chromatography (TLC). For sterol analysis, the lipid extract was loaded into TLC silica plates (Si 60F254s; LiChrospher, Germany) and separated using a solvent system containing hexane:ether:acetic acid (80:40:2, vol:vol:vol) solvent. The plate was sprayed with a solution of 50 mg ferric chloride ($FeCl_3$) in a mixture of 90 ml water, 5 ml acetic acid, and 5 ml sulfuric acid. Sterol spots were identified by the appearance of a purple color after heating the plates at 100 °C for 3–5 min. For phospholipid identification, the dry residue was suspended in 90% methanol. After centrifugation, aliquots of the supernatant (typically 100 μl) were injected onto a reverse phase HPLC column (Supleco Ascentis® Express, C18, 150 × 2.1 mm) equilibrated in buffer A (methanol/water, 95/5, v/v, containing 1 mM ammonium acetate), and eluted (100 μl/m) with an increasing concentration of buffer B (chloroform/water, 500/0.2, v/v, containing 1 mM ammonium acetate; min/%B, 0/0, 5/0, 55/100). The effluent from the column was split, with a portion (about 70%) directed to a fraction collector (1 min fractions) and the remainder (about 30%) passed to an Ionspray® source connected to a triple quadrupole mass spectrometer (PE Sciex API III$^+$) operating in the precursor (parent) scan mode in which Q1 was scanned (0.3 Da step, 6.7 s/scan, orifice 50 V), the collision chamber was flooded with argon gas (collision gas thickness setting at 120), and Q3 was set to transmit ions at *m/z* 184.1 Da.

To confirm assignments made from the LC/MS/MS data, and to further define the composition of the phosphocholine lipids in the sample, positive and negative ion mass spectra were recorded off-line by direct injection of aliquots of fractions collected during LC/MS/MS. Fractions 24–29 were pooled, and aliquots (20 μl) were injected into a stream of methanol/chloroform (4/1, v/v; 50 μl/m) entering the Ionspray® source of the mass spectrometer, before and following the addition of formic acid (1 μl, positive ion mode) and triethylamine (1 μl, negative ion mode). These experiments were done with the mass spectrometer operating in either the normal (Q1 scan range *m/z* 200–1500, orifice 70 V, 4.6 s/scan), or the tandem mass spectrometric modes (precursor and fragment scan modes). In particular, negative ion fragment scans at high orifice voltage (120) and relatively high collision gas density (CGT setting 150), were used to assign phosphocholine fatty acid substituents after the addition of triethylamine. These experiments were done using methods originally described by Jensen et al. (1986). Putative parent ions for these experiments were assigned from the results of the LC/MS/MS parent ion data, and confirmed by the results from the direct injection analyses. The parent ions were assigned as 16 Da lighter than that determined experimentally, with the loss of 15 Da predicted to result from source fragmentation at high orifice voltage (loss of one nitrogen methyl group), and 1 Da loss resulting from abstraction of the proton attached to the phosphorous oxygen under basic conditions. Data was analyzed with instrument-supplied software (MacSpec version 3.3), and optimal conditions for the experiments were established using authentic di-palmitoylphosphatidyl choline, heptadecanoyl-lyso-phosphatidyl choline and di-heptanoylphosphatidyl choline standards.

2.5. GXM capture ELISA

A 96-well polystyrene plate was coated with the capture IgM mAb 2D10 (10 μg/ml) for 1 h and then blocked with 1% bovine serum albumin for. The plates were then incubated with GXM fractions from vesicle samples, obtained by precipitation with a mixture of chloroform and methanol (see item lipid analysis). After three washing cycles with TBS 0,05% Tween 20, the plates were incubated with an IgG1 to GXM (mAb 18B7, 2 μg/ml) for 1 h at room temperature. Positive reactions were developed by incubation with an alkaline phosphatase-conjugated anti-IgG1 followed by reaction with *p*-nitrophenyl phosphate disodium hexahydrate for 30 min. Absorbance values were measured at 405 nm in a microplate reader.

3. Results and discussion

Electron microscopy procedures for the study of the *C. neoformans* biology are complex because this fungal species is surrounded by a polysaccharide capsule, which is attached to a thick cell wall. The combination of a large capsule and thick cell wall can slow fixation process resulting in cellular degradation. Hence, obtaining high quality micrographs of cryptococcal cells can take some trial and error to identify the best conditions for fixation. In this context, the commonly used protocols for immunogold analysis of *C. neoformans* usually include particular steps, such as partial digestion of the cell wall (Yoneda and Doering, 2006), to ensure a more efficient process of embedding and consequent preservation of intracellular compartments. Unfortunately, these procedures are often accompanied by loss of surface components and, consequently, produce micrographs that convey limited information on the cryptococcal cellular anatomy (Yamaguchi et al., 2005). The advantages of using cryosectioning techniques have already been demonstrated in the model yeast *S. cerevisiae*, where protocols based on the method of Tokuyasu (1973) resulted in high resolution images with well preserved cellular structures and efficient immunogold labeling (Griffith et al., 2008). The general procedures to prepare biological samples according to this method include fixation, infiltration/cryoprotection and rapid freezing in liquid nitrogen.

In the current study cryoultramicrotomy allowed the generation of well-preserved *C. neoformans* sections (Fig. 1). Intracellular compartments such as the nucleus, vacuoles, mitochondria, cell wall and capsule were clearly distinguishable. Even in the absence of a post-fixation step with OsO_4, lipid bilayers were well preserved and easily discernible, as evidenced in nuclear compartments and mitochondrial lamellas (Fig. 1). In addition to the better known organelles, other subcellular structures were evident, including reticular membrane clusters close to the plasma membrane (Fig. 1C, black arrows). These compartments showed morphological similarities to structures derived from the endoplasmic reticulum, although their peripheral position inside the cell suggested early endosomes (Gould and Lippincott-Schwartz, 2009). A membranous compartment that resembled the endoplasmic reticulum was also visible in the proximity of nucleus (Fig. 1C). Finally, vesicular structures manifesting electron dense contents were also apparent (Fig. 1B). These structures had similarities to intermediate/late endosomal compartments called acidosomes (Allen et al., 1993) and also to mammalian melanosomes at different maturation stages (Raposo and Marks, 2007). These compartments, which were consistently observed in our preparations, are shown in more detail in Fig. 2. Similar intracellular structures that contained GXM were recently described by Yoneda and Doering using a secretion-deficient mutant of *C. neoformans* (Yoneda and Doering, 2009). However, the electron dense compartments observed in our model do not display such intense GXM labeling (Fig. 2), as described in that study for *C. neoformans* cells. In our model, some of the intracellular compartments also contained internal vesicles (Fig. 1B and C) that show similarities

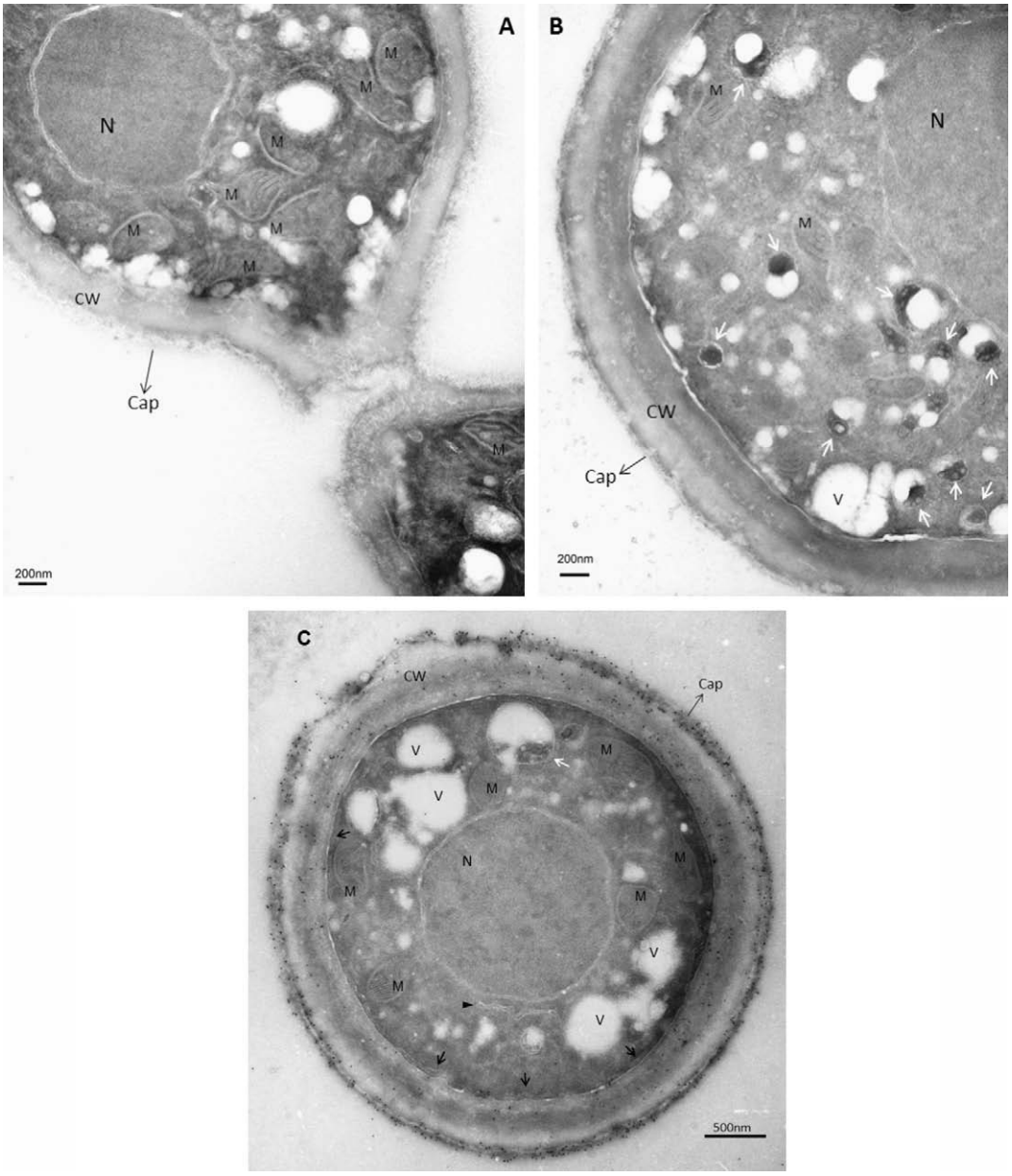

Fig. 1. Anatomy of the *C. neoformans* ultrastructure. *C. neoformans* cells were grown to stationary phase and prepared for EM as described in Section 2. Several organelles were distinguished, including nucleus (N), vacuoles (V), mitochondria (M), cell wall (CW) and a compacted capsule (Cap). The existence of lamellar structures with unknown cellular roles (black arrows) is suggested, as well as of vesicular electron dense compartments (white arrows). Black arrow heads indicate putative endoplasmic reticulum. Unlabeled cells (A and B) and cells stained for the presence of GXM (C) are shown.

to the so-called multivesicular bodies (MVBs) found in mammalian cells (Gruenberg and Stenmark, 2004). The existence of MVBs in *C. neoformans* was previously suggested using different techniques (Rodrigues et al., 2008; Takeo et al., 1973), although differences in morphology and electron density were noticed by comparing the currently described results with those from previous studies.

Intracellular sites manifesting immunogold staining with mAb to GXM were usually found in association with membranous structures (Fig. 3). Quantification of immunogold labeling in intracellular compartments revealed that approximately 70% of the antibody-binding sites were membrane-associated. On the basis of this reactivity we tentatively assigned these areas as sites of GXM synthesis/transport. Membrane compartments resembling vesicles carrying GXM were repeatedly observed (Fig. 3), as well as structures resembling mammalian MVBs (Fig. 3C) and peripheral reticular clusters resembling endosomes (Fig. 3E). Since GXM staining was often found in close association with the lipid bilayer, we hypothesize that polysaccharide-binding proteins could be inserted in these lipid bilayers functioning as transient GXM anchors, which still remains to be investigated. Considering that the size of the complex gold-labeled antibody to GXM may in some instances exceed the diameter of those structures, we cannot rule out the possibility that they are located in neighboring intracellular regions, although previous data indeed demonstrate that GXM associated with secretory vesicles (Casadevall et al., 2009; Feldmesser et al., 2001; Garcia-Rivera et al., 2004; Rodrigues et al., 2007; Yoneda and Doering, 2006).

The intracellular, electron dense compartments described by Yoneda and Doering (2009) were called *sav1* bodies, since they were most prominently observed in *C. neoformans* cells with

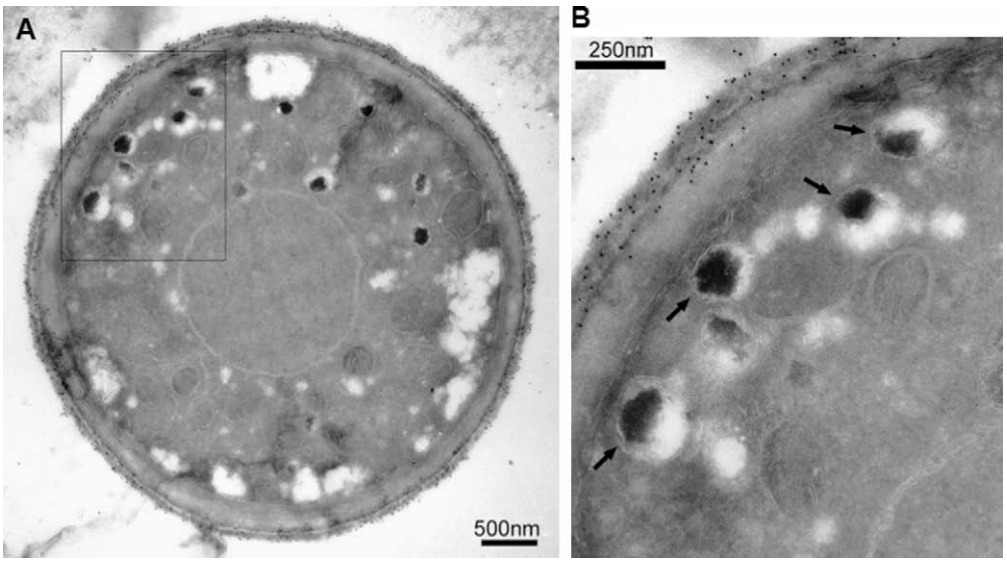

Fig. 2. Electron dense organelles are present in *C. neoformans*. The boxed area shown in A is shown in higher magnification in B. Arrows indicate the electron dense bodies. The composition of these electron dense structures is unknown. Cell surface labeling represents reactivity of cryptococcal components with mAb18B7.

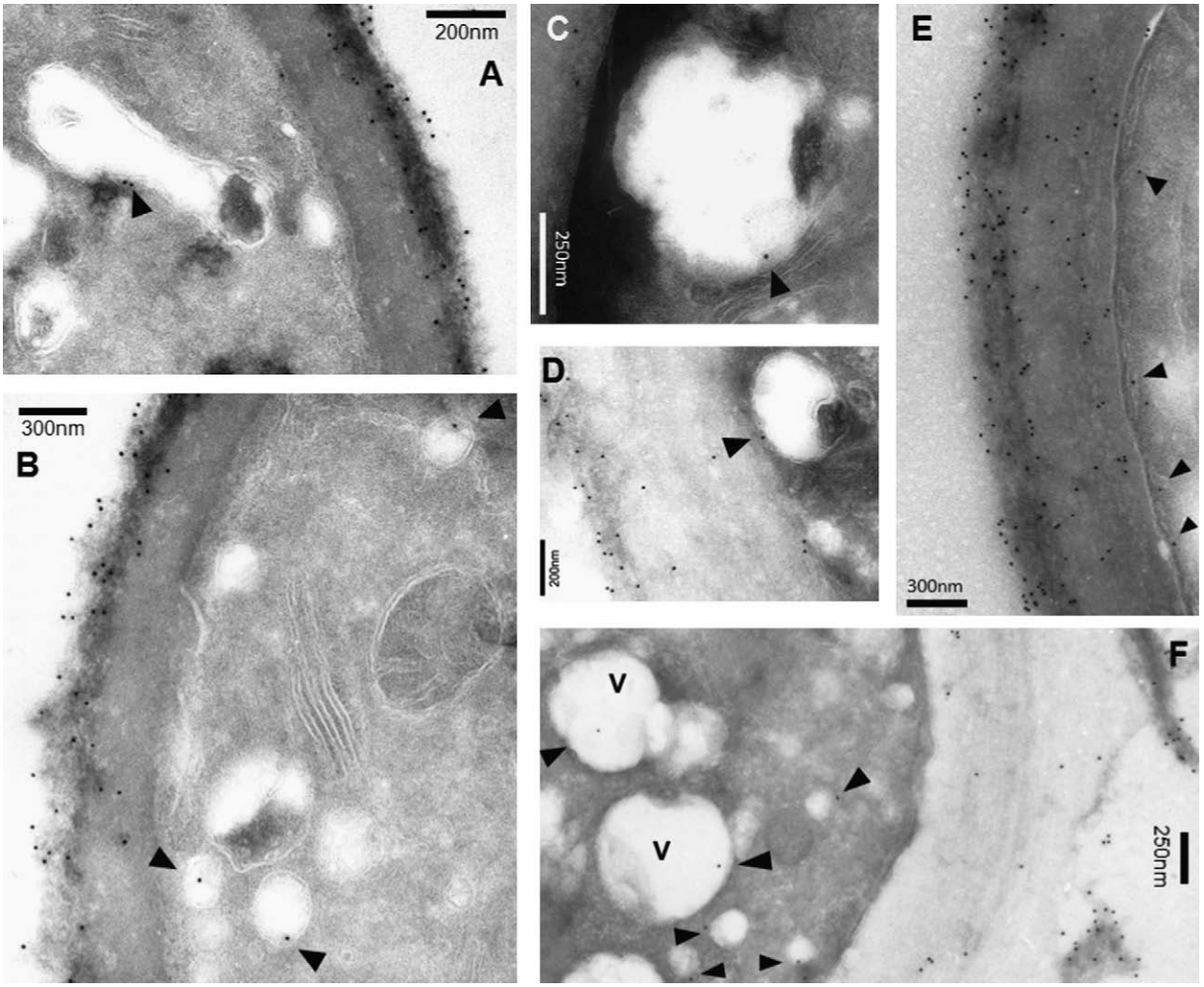

Fig. 3. Cryptococcal GXM is found in association with vesicles and membranous structures. Cells were labeled with GXM binding mAb 18B7. GXM is generally detected in association with lipid bilayers. In A and D, the arrowhead indicates that GXM can be localized inside vesicles that also present an electron dense content. In B and F, GXM seems to be localized inside small cytoplasmic vesicle carriers. In F GXM is also presented inside the vacuole (V). In C, an unknown structure containing internal vesicles also displays mAb18B7 labeling, as well as reticular unknown structures close to the plasma membrane displayed in E.

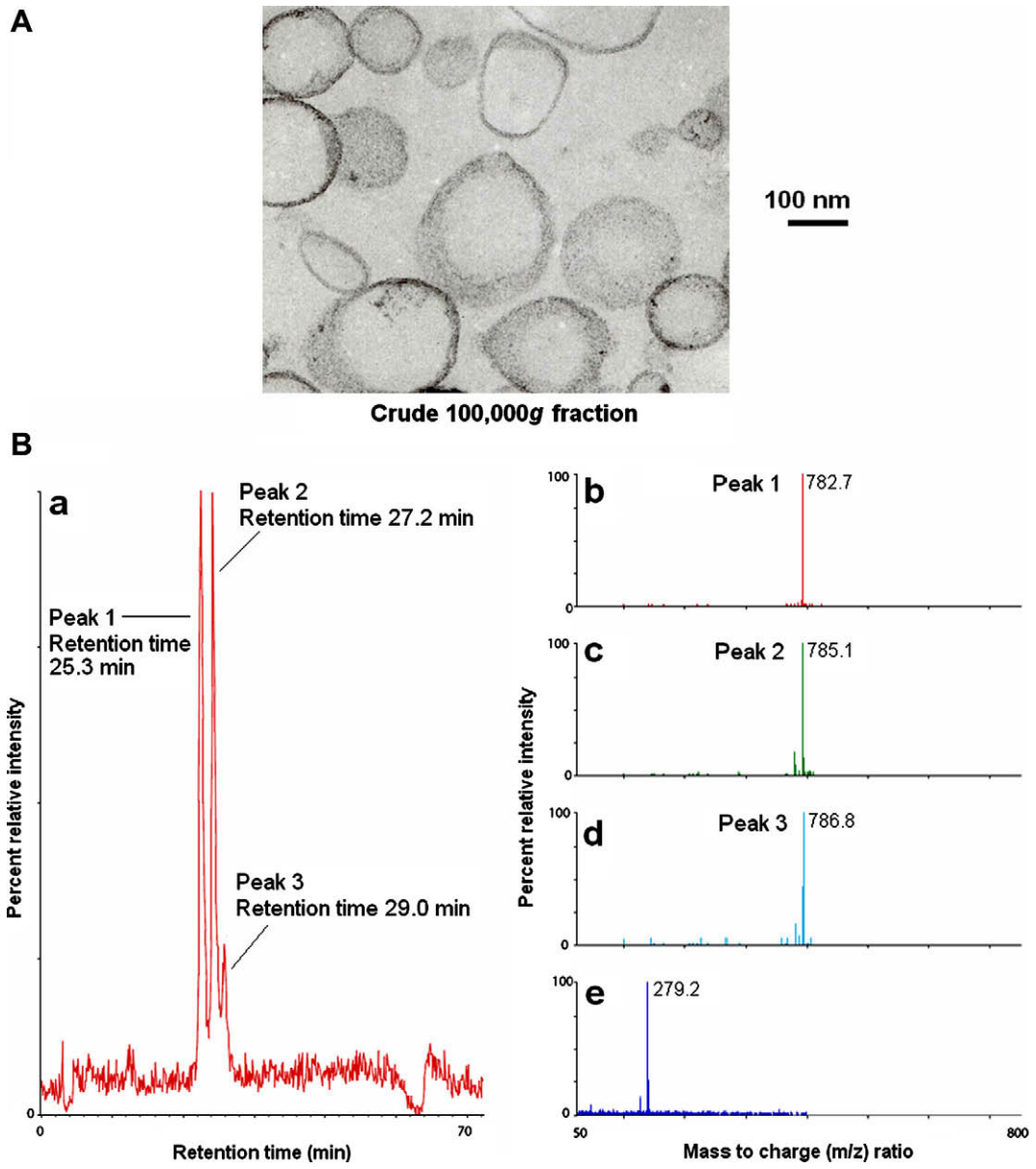

Fig. 4. Analysis of phosphatidylcholine (PC) in extracellular vesicles. (A) Transmission electron microscopy showing vesicle morphology in 100,000*g* fractions isolated from culture supernatants. (B) Characterization of PC in vesicle fractions: (a) total ion current LCMSMS chromatogram obtained following injection of the crude vesicle preparation onto a reverse phase column as described in Section 2. The mass spectrometer was operated in the MS/MS precursor (parent) scan mode in which the *m/z* value of parent ions that give rise to the *m/z* 184.1 fragment are recorded, (b–d) electrospray ionization mass spectra of the three peaks shown in Figure A (Peaks 1–3, MS/MS positive ion precursor (parent) scan mode, precursors of *m/z* 184.1) and (e) negative ion electrospray mass spectrum of the fragments derived from an *m/z* 766.7 parent ion under MS/MS conditions after addition of triethylamine as described in Section 2. Calculated values: $C_{44}H_{81}NO_8P$ 782.570 Da; $C_{44}H_{83}NO_8P$ 784.586 Da; $C_{44}H_{85}NO_8P$ 786.601 Da; $C_{18}H_{31}O_2$ 279.232 Da.

defective expression of sav1p, a putative small GTPase involved in post-Golgi secretion. The compartments observed in our model are apparently distinct from the *sav1* bodies, since they did not manifest significant reactivity with an antibody to GXM, despite morphological similarities (Figs. 2 and 3A and D). The presence of GXM in vacuoles (Fig. 3F) could be related to secretion mechanisms initiated by endocytosis or to mechanisms of GXM recycling. In fact, the GXM catabolic process is poorly understood and so far hydrolytic enzymes able to cleave GXM have not been reported in *C. neoformans* (Bose et al., 2003; Zaragoza et al., 2009).

Conventional procedures for TEM usually generate artificially compacted cell wall structures, probably because of dehydration steps. In our model, as well as in a previous study, cryoultramicrotomy procedures allowed the observation of structures that illustrate the thickness and complexity of the cell wall. As suggested in previous studies with fungal cells (Soragni et al., 2001), clear distinctions between regions of different electron densities were observed (Figs. 1B,C and 3F), which may be related to the description of secondary cell walls during stationary growth of *C. neoformans* (Farkas et al., 2009). Most of the cellular sites recognized by the mAb to GXM were found in association with the cell wall or within the capsular region (Fig. 1C), corroborating with previous observations (Yoneda and Doering, 2006).

GXM has been proposed to be exported to the extracellular space in secretory vesicles, suggesting an association of lipids and polysaccharides in *C. neoformans* (Rodrigues et al., 2007). This notion is supported by our current observations in the cryptococcal cytoplasm. Glucosylceramide and sterols were previously

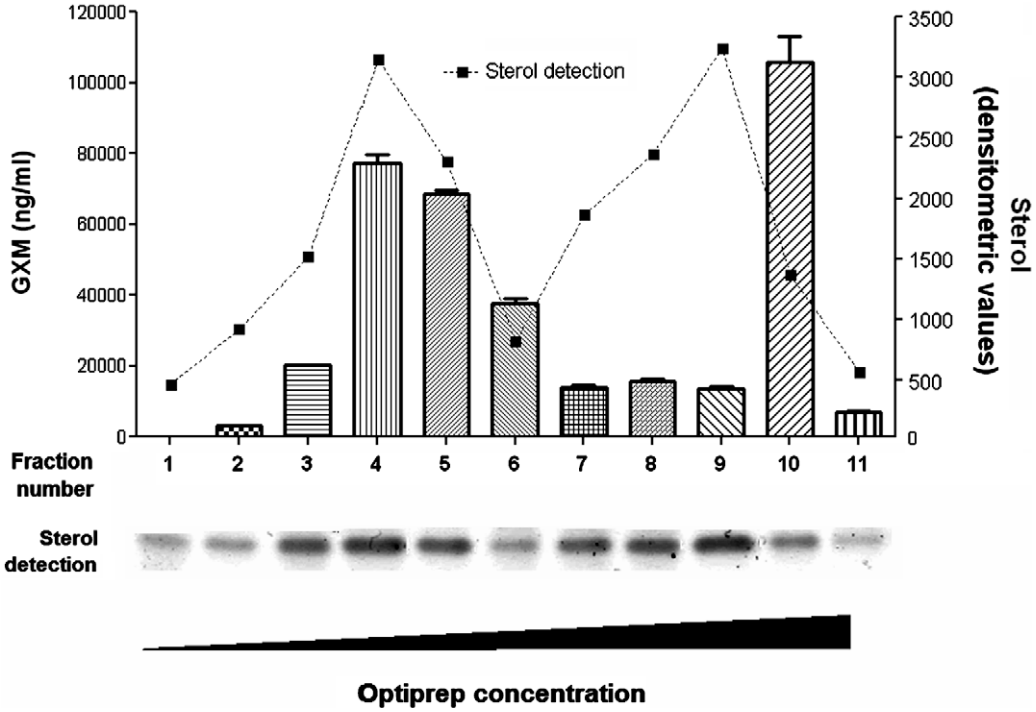

Fig. 5. Fractionation of *C. neoformans* extracellular vesicles. A crude preparation of extracellular vesicles was fractionated in a 6–18% Optiprep velocity gradient. Eleven fractions were recovered and individually tested for the presence of GXM by ELISA and ergosterol by thin-layer chromatography (TLC). TLC bands (sterol detection) were quantified by densitometry. Sterol distribution in fractions (dotted line) and GXM content (bars) are shown.

characterized as membrane components of the *C. neoformans* vesicles (Rodrigues et al., 2007), but other lipid components of GXM-containing vesicles are still unknown. To evaluate the relationship of lipids with GXM export, we first tested whether extracellular vesicle samples contained GXM by ELISA. Vesicles obtained from encapsulated cells reacted with the antibody to GXM, while vesicles from an acapsular mutant manifested a much lower reactivity (data not shown). These results were in agreement with those described by Rodrigues and co-workers (2007) and support the hypothesis that the major capsular polysaccharide of *C. neoformans* associates with lipids for extracellular export. Since phospholipids are major membrane constituents in most cells, but also in extracellular vesicles of the fungal pathogen *Histoplasma capsulatum* (Albuquerque et al., 2008), we evaluated whether the crude fraction of GXM-containing vesicles contained this class of molecules.

To ensure that lipid characterization did not include membrane fractions from non-vesicular structures, the integrity and morphology of 100,000*g* fractions isolated from culture supernatants was analyzed by TEM. Vesicles in these fractions showed typical bilayered membranes that generally formed round compartments in the size range of 50–300 nm (Fig. 4A), which is in agreement with previous reports on the morphological characterization of fungal extracellular vesicles (Rodrigues et al., 2008; Eisenman et al., in press). These fractions were then used for phospholipid extraction.

Cryptococcal phospholipids include phosphatidylinositol, lysophosphatidyl ethanolamine, cardiolipin, glycophospholipids, lysophosphatidyl choline, phosphatidic acid, phosphatidyl ethanolamine and phosphatidyl choline (PC) (Rawat et al., 1984). PC was the major phospholipid component of *C. neoformans* cellular membranes (Rawat et al., 1984), so this molecule was selected as a potential candidate component of cryptococcal vesicles. Samples were subjected to precursor ion scanning of the *m/z* 184.1 fragment. This ion corresponds to phosphorylcholine, and therefore represents a molecular marker for the presence of PC. Control samples consisted of LCMS analysis of the solvent alone, which showed no significant peaks. From the vesicle samples, three strong peaks were observed eluting between 24 and 29 min (Fig. 4B, panel a). These peaks revealed parent masses of 782.7, 784.6 and 786.8 Da (Fig. 4B, panel b–d). LCMS analysis of two different samples produced essentially identical results (data not shown). Fractions eluting between 24 and 29 min were pooled and examined by direct flow-injection MS and MS/MS. Fragmentation of the peak at *m/z* 782.7 generated a strong signal at *m/z* 184 (data not shown), confirming the occurrence of PC. To analyze fatty acid components, negative MS/MS analysis was performed after addition of triethylamine. Analysis of the peaks at *m/z* 782.7 and 784.6 revealed the presence of related fragments at *m/z* 279.2 (Fig. 4B, panel e) and 281.0 (not shown), consistent with the presence of, respectively, fatty acids corresponding to C18:2 and C18:1. The peak at *m/z* 786.8 did not yield a significant response probably because of limitations in amount of sample (data not shown).

In our study, intracellular GXM-containing vesicles were repeatedly observed (Fig. 3), as well as several unlabeled vesicular structures (Figs. 1C and 2). In this context, we evaluated whether the distribution of GXM in extracellular vesicles could reflect the results observed in cellular structures. Fractionation of vesicle samples by gradient centrifugation followed by lipid and polysaccharide analysis revealed a previously unknown compositional profile of extracellular fungal vesicles (Fig. 5). Sterol analysis was used to track membrane-containing fractions, since ergosterol has been characterized as an easily detectable component of vesicular membranes (Rodrigues et al., 2007). Phospholipid analysis in gradient fractions was not pursued due to poor sensitivity for lipid detection in chromatographic methods.

Ergosterol was detected in all fractions obtained after ultracentrifugation. GXM-containing fractions of different densities (fractions 4–6 and 10), as well as sterol-containing fractions that showed virtually no reactivity with an antibody to GXM (fractions 1–2 and 7–9), were observed. In some cases, the amounts of GXM and sterols in gradient fractions were directly correlated

(e.g. fractions 4–6), but fractions with lower ergosterol content and high GXM density were also observed (e.g. fraction 10). These results are consistent with previously noted heterogeneity in vesicle size and composition (Albuquerque et al., 2008; Rodrigues et al., 2008) and indicate that some vesicles are preferentially associated with polysaccharide transport while others contain no GXM, as noted in prior immunogold labeling studies (Rodrigues et al., 2007). The observation of extracellular vesicle fractions with such different properties indicate that the cellular events required for vesicle biogenesis are multiple and complex, as previously suggested by morphological analysis of cryptococcal extracellular vesicles (Rodrigues et al., 2008). Our results add to the evolving theme an intimate and intriguing association between lipid and polysaccharide components in *C. neoformans* capsule (Nicola et al., 2009; Sebolai et al., 2007, 2008).

In this work we report the use of two methodological approaches for studying the process of polysaccharide synthesis and transport: (1) a cryosectioning protocol for *C. neoformans*, which allowed a distinguished resolution of the fungal cytoplasmic content and surface structures, and (2) a technique for fractionating vesicles that separates them into GXM- and non-GXM containing groups. The cryosectioning EM method allowed us to discern in more detail the distribution of GXM inside the cell. The vesicle fractionation approach should allow finer resolution studies of vesicle composition and content by biochemical and mass spectrometry analysis. The results of these studies revealed new details for the mechanisms required for polysaccharide traffic and raise new questions about this complex cellular process. Of particular interest was the association of GXM with membrane structures suggesting that this polysaccharide is synthesized in close proximity to lipids, possibly by anchored enzymes. The possibility of combining cryoultramicrotomy with other less invasive methods such as high pressure freezing followed by freeze substitution and electron tomography could potentially generate new information for the study of still unknown cell biology attributes of cell-wall containing pathogens.

Acknowledgements

A.C. was supported by NIH Grants AI33774, HL59842, AI33142, and AI52733. M.L.R., L.N. and K.M. were supported by Grants from the Brazilian agencies CNPq and FAPERJ. We thank Leslie Gunther and the Analytical Imaging Facility team at Albert Einstein College of Medicine for their assistance with the electron microscopy experiments. We also thank Jorge José Jó B. Ferreira for helpful discussions. DLO is a PhD student at Instituto de Bioquímica Médica, UFRJ.

References

Albuquerque, P.C. et al., 2008. Vesicular transport in *Histoplasma capsulatum*: an effective mechanism for trans-cell wall transfer of proteins and lipids in ascomycetes. Cell Microbiol. 10, 1695–1710.

Allen, R.D. et al., 1993. Acidosomes: recipients of multiple sources of membrane and cargo during development and maturation. J. Cell Sci. 106 (Pt 1), 411–422.

Bose, I. et al., 2003. A yeast under cover: the capsule of *Cryptococcus neoformans*. Eukaryot. Cell 2, 655–663.

Cantin, R. et al., 2008. Discrimination between exosomes and HIV-1: purification of both vesicles from cell-free supernatants. J. Immunol. Methods 338, 21–30.

Casadevall, A. et al., 2009. Vesicular transport across the fungal cell wall. Trends Microbiol. 17, 158–162.

Eisenman, H.C., Frases, S., Nicola, A.M., Rodrigues, M.L., Casadevall. A., Vesicle-associated melanization in *Cryptococcus neoformans*. Microbiology, in press, doi:10.1099/mic.0.032854-0.

Farkas, V. et al., 2009. Secondary cell wall formation in *Cryptococcus neoformans* as a rescue mechanism against acid-induced autolysis. FEMS Yeast Res. 9, 311–320.

Feldmesser, M. et al., 2001. Dynamic changes in the morphology of *Cryptococcus neoformans* during murine pulmonary infection. Microbiology 147, 2355–2365.

Folch, J. et al., 1957. A simple method for the isolation and purification of total lipides from animal tissues. J. Biol. Chem. 226, 497–509.

Garcia-Rivera, J. et al., 2004. *Cryptococcus neoformans* CAP59 (or Cap59p) is involved in the extracellular trafficking of capsular glucuronoxylomannan. Eukaryot. Cell 3, 385–392.

Gould, G.W., Lippincott-Schwartz, J., 2009. New roles for endosomes: from vesicular carriers to multi-purpose platforms. Nat. Rev. Mol. Cell Biol. 10, 287–292.

Griffith, J. et al., 2008. A cryosectioning procedure for the ultrastructural analysis and the immunogold labelling of yeast *Saccharomyces cerevisiae*. Traffic 9, 1060–1072.

Gruenberg, J., Stenmark, H., 2004. The biogenesis of multivesicular endosomes. Nat. Rev. Mol. Cell Biol. 5, 317–323.

Jensen, N.J. et al., 1986. Fast atom bombardment and tandem mass spectrometry of phosphatidylserine and phosphatidylcholine. Lipids 21, 580–588.

McClelland, E.E. et al., 2005. Coping with multiple virulence factors: which is most important? PLoS Pathog. 1, e40.

Monari, C. et al., 2008. Capsular polysaccharide induction of apoptosis by intrinsic and extrinsic mechanisms. Cell Microbiol. 10, 2129–2137.

Nicola, A.M. et al., 2009. Lipophilic dye staining of *Cryptococcus neoformans* extracellular vesicles and capsule. Eukaryot. Cell. 8, 1373–1380.

Panepinto, J. et al., 2009. Sec6-dependent sorting of fungal extracellular exosomes and laccase of *Cryptococcus neoformans*. Mol. Microbiol. 71, 1165–1176.

Raposo, G., Marks, M.S., 2007. Melanosomes – dark organelles enlighten endosomal membrane transport. Nat. Rev. Mol. Cell Biol. 8, 786–797.

Rawat, D.S. et al., 1984. Lipid composition of *Cryptococcus neoformans*. Microbiologica 7, 299–307.

Rodrigues, M.L. et al., 2008. Extracellular vesicles produced by *Cryptococcus neoformans* contain protein components associated with virulence. Eukaryot Cell. 7, 58–67.

Rodrigues, M.L. et al., 2007. Vesicular polysaccharide export in *Cryptococcus neoformans* is a eukaryotic solution to the problem of fungal trans-cell wall transport. Eukaryot. Cell. 6, 48–59.

Rodrigues, M.L. et al., 2000. Human antibodies against a purified glucosylceramide from *Cryptococcus neoformans* inhibit cell budding and fungal growth. Infect Immunol. 68, 7049–7060.

Sebolai, O.M. et al., 2007. 3-Hydroxy fatty acids found in capsules of *Cryptococcus neoformans*. Can. J. Microbiol. 53, 809–812.

Sebolai, O.M. et al., 2008. The influence of acetylsalicylic acid on oxylipin migration in *Cryptococcus neoformans* var. neoformans UOFS Y-1378. Can. J. Microbiol. 54, 91–96.

Slot, J.W., Geuze, H.J., 2007. Cryosectioning and immunolabeling. Nat. Protoc. 2, 2480–2491.

Soragni, E. et al., 2001. A nutrient-regulated, dual localization phospholipase A(2) in the symbiotic fungus Tuber borchii. EMBO J. 20, 5079–5090.

Steenbergen, J.N. et al., 2001. *Cryptococcus neoformans* interactions with amoebae suggest an explanation for its virulence and intracellular pathogenic strategy in macrophages. Proc. Nat. Acad. Sci. USA 98, 15245–15250.

Takeo, K. et al., 1973. Fine structure of *Cryptococcus neoformans* grown in vitro as observed by freeze-etching. J. Bacteriol. 113, 1442–1448.

Tokuyasu, K.T., 1973. A technique for ultracryotomy of cell suspensions and tissues. J. Cell Biol. 57, 551–565.

Vecchiarelli, A., 2007. Fungal capsular polysaccharide and T-cell suppression: the hidden nature of poor immunogenicity. Crit. Rev. Immunol. 27, 547–557.

Wills, E.A. et al., 2001. Identification and characterization of the *Cryptococcus neoformans* phosphomannose isomerase-encoding gene, MAN1, and its impact on pathogenicity. Mol. Microbiol. 40, 610–620.

Yamaguchi, M. et al., 2005. Safe specimen preparation for electron microscopy of pathogenic fungi by freeze-substitution after glutaraldehyde fixation. Nippon Ishinkin Gakkai Zasshi 46, 187–192.

Yoneda, A., Doering, T.L., 2006. A eukaryotic capsular polysaccharide is synthesized intracellularly and secreted via exocytosis. Mol. Biol. Cell 17, 5131–5140.

Yoneda, A., Doering, T.L., 2009. An unusual organelle in *Cryptococcus neoformans* links luminal pH and capsule biosynthesis. Fungal Genet. Biol. 46, 682–687.

Zaragoza, O. et al., 2009. The capsule of the fungal pathogen *Cryptococcus neoformans*. Adv. Appl. Microbiol. 68, 133–216 (Chapter 4).